Asian Journal of Chemistry; Vol. 24, No. 8 (2012), 3406-3410

ASIAN JOURNAL OF CHEMISTRY

www.asianjournalofchemistry.co.in

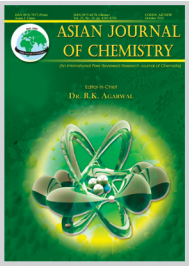

The First Principles Study of Electronic and Optical Properties of TiO_2 Isomers

SHUFANG WU[1,2,*], TIANMO LIU[1,2], WENYONG QIN[1,2], CHENG CHEN[1,2], XIAOFEI LEI[1,2] and WEN ZENG[1,2]

[1]College of Materials Science and Engineering, Chongqing University, Chongqing 400044, P.R. China
[2]National Engineering Research Center for Magnesium Alloys, Chongqing University, Chongqing 400044, P.R. China

*Corresponding author: Tel: +86 13648320182; E-mail: wushufangwxce@yahoo.com.cn

(*Received*: 1 July 2011; *Accepted*: 6 March 2012) AJC-11153

The electronic and optical properties of three TiO_2 isomers are systematically investigated by the first-principles calculations, using generalized gradient approximation based on the density-functional theory. Such electronic and optical properties as optimized crystal structures, band structures, partial and total densities of states, reflectivity, absorption coefficient, refractive index, energy-loss spectrum and dielectric function is calculated. It was found that the electronic parameters for the three isomers are almost similar and our calculated results are in excellent agreement with experimental values and other previous theoretical calculations. At the same time, both of the valence band and conduction band contain contributions from the states of O *p* and Ti *d*, which indicates hybridization between these states. In addition, the absorption peaks correspond to the band-to-band transitions from O *p* states to Ti *d* states, while the states of O *p* and the Ti *d* play a major role in these optical transitions and the values of $\varepsilon_1(0)$ increase as the band-gap decreases.

Key Words: The first principle, TiO_2, Electronic properties, Optical properties.

INTRODUCTION

Titanium dioxide (TiO_2) has three isomers *i.e.*, rutile-TiO_2, anatase-TiO_2 and brookite-TiO_2. For the past several decades, TiO_2 has been extensively studied for its excellent performance as solar cell[1], white pigment[2], photo catalyst[3] and water purification[4].

There have been many studies of the electronic and structural properties of TiO_2, both of experimental[5,6] and theoretical aspects[7-9]. Experimentally, the electronic structure of rutile-TiO_2 has been studied by X-ray photoemission spectroscopy (XPS)[10] and electron-energy-loss spectroscopy (EELS)[6]. Xu *et al.*[11] found that the spectral responses relevant to optical absorption of P-doped TiO_2 powders shift to the visible light region and the corresponding absorption edge shifts to 480 nm, while the optimum P content in their experiments is 16.7 % (mol). Weng *et al.*[12] studied the Co-doped anatase-TiO_2 within the local-spin-density approximation (LSDA) and they found that the doped Co concentrations from 0.0417 to 0.0625 have only a little effect on them, but the oxygen vacancy and its distribution in the stem have much larger influences. Asahi *et al.*[13] and Baizaee *et al.*[14] have investigated detailed electronic and optical properties of TiO_2 using the full potential linearized augmented plane wave (FP-LAPW) method.

In spite of all these studies, not much is known about the optical response of TiO_2. It is therefore critical to have a systematic theoretical investigation on the electronic and optical properties of TiO_2. Furthermore, despite that many previous theoretical studies employed either local-spin-density approximation or full potential linearized augmented plane wave, it is still necessary to use other the first-principles method such as the generalized gradient approximation (GGA) to provide interpretations for experimental data.

It is very interesting to obtain the optical response, such as the dielectric function and absorption in the optical frequency range and inspect the available band gaps data for these compounds in detail. In this work, we investigated the optimum lattice parameters, the electronic and optical properties of TiO_2. This paper is organized as follows. A brief description of the calculation method is given here, the results of calculations as well as the discussions are presented.

EXPERIMENTAL

The computational calculations have been performed using the Vienna *ab initio* simulation package (VASP) within the framework of density-functional theory (DFT)[15,16] plane-wave pseudopotential method, which uses a plane wave basis set and projector augmented wave (PAW)[17] potentials and was used for electron-ion interactions and the generalized gradient approximation of Perdew *et al.* (PW91)[18] was employed to describe the exchange-correlation functional. The convergence with respect to the k point mesh and cut-off energy for the plane wave basis set was carefully checked. The single-

particle Kohn-Sham wave function was expanded using plane waves with different cut-off energies depending on the calculated systems. Sampling of irreducible Brillouin zone was performed with a regular Monkhorst-Pack grid of special k points[19] and electronic occupancies were determined according to the Methfessel-Paxton scheme[20]. Total energies were calculated using the linear tetrahedron method with Blöchl corrections[21,22], which eliminates broadening-related uncertainties. All atoms were fully relaxed using the conjugate gradient algorithm[23] until the magnitude of the Hellmann-Feynman force[24] on each atom converged to less than 0.05 eV/Å, yielding optimized structures.

RESULTS AND DISCUSSION

Geometric structure: The schematic models of the three TiO_2 isomers are shown in Fig. 1. We verified accuracy of the computational methods by performing bulk calculations. It is known that rutile-TiO_2, one of the most common TiO_2 isomers, belongs to the tetragonal P42/mnm space group with a = 4.593 Å and c = 2.959 Å[25]; anatase-TiO_2 also has a tetragonal structure but within the I41/amd space group (a = 3.784 Å and c = 9.515 Å)[25]; brookite-TiO_2 belongs to the orthorhombic Pbca space group with a = 5.163 Å, b = 9.159 Å and c = 5.439 Å[26]. Bulk properties were calculated using a cut-off energy of 450 eV, 2 × 2 × 4 k points for rutile-TiO_2, 4 × 4 × 2 k points for anatase-TiO_2 and 4 × 2 × 4 k points for brookite-TiO_2, which converges total energies to less than 1 meV/atom. The calculated optimum lattice constants of bulk rutile-TiO_2 are a = 4.639 Å and c = 2.989 Å, 101 % of the experimental values; while those of bulk anatase-TiO_2 are a = 3.832 Å and c = 9.634 Å, 101.25 % of the experimental values; those of bulk brookite-TiO_2 are a = 5.215 Å, b = 9.251 Å and c = 5.493 Å, 101 % of the experimental values. In addition, our calculated values are in excellent agreement with other reported results.

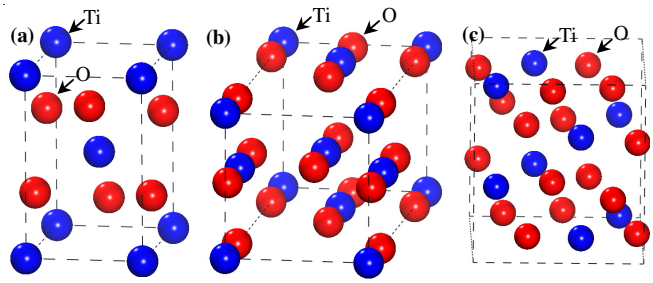

Fig. 1. Schematic model of (a) rutile-TiO_2, (b) anatase-TiO_2 and (c) brookite-TiO_2

Electronic properties: Fig. 2 shows the calculated band structure for the three isomers of TiO_2. For rutile-TiO_2, the calculated energy band gap of 1.847 eV is direct at G, which is much smaller than the experimental value of 3.0 eV[27,28] and the value of 3.89 eV calculated using the augmented spherical wave band structure approach (ASW) and self-consistent field scattered wave molecular orbital cluster (Xa-SW) methods, as reported by Mishra *et al.*[29]. However, it is close to the calculated value of 2.18 eV reported by Glassford *et al.*[7] and the 1.87 eV reported by Shao *et al.*[30]. Deviation from the experimental value is attributed to the well-known drawback of the DFT[31,32], namely by not taking into account the discontinuity in the exchange-correlation potential[33].

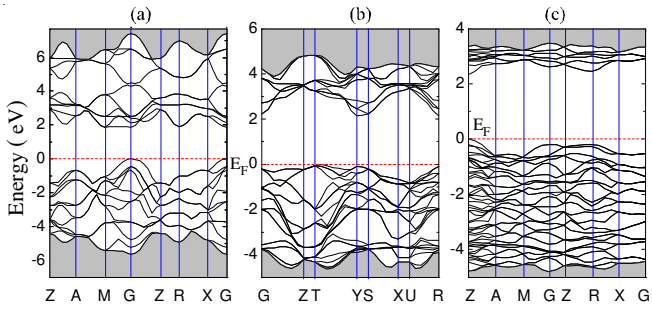

Fig. 2. Energy band structure of (a) rutile-TiO_2, (b) anatase-TiO_2 and (c) brookite-TiO_2 along major symmetric directions. The horizontal and dashed lines represent the Fermi level (EF)

Unlike rutile-TiO_2, the calculated minimal band gap of 2.14 eV for anatase-TiO_2 is indirect. However, the energy of the maximum of the valence band at the G point is only about 0.1 eV lower than the valence band top and this allows treating it as an almost direct-gap compound. The calculated band gap in this work is 1.19 eV below the experimental value of 3.0 eV calculated using generalized gradient approximation with the CASTEP program, reported by Yin *et al.*[34], 0.2 eV larger than that of rutile-TiO_2. However, it agrees well with previously reported theoretical estimations, the calculated value of 2.13 eV reported by Brik *et al.*[35] and 2.0 eV reported by Asahi *et al.*[13]. The calculation values are acceptable for comparison, as electronic structure calculation within DFT usually underestimates band gaps[36].

We are not aware of any reported experimental data for brookite-TiO_2. However, we expect the electronic structure of brookite-TiO_2 to be similar to that of anatase-TiO_2 because there is only minor difference in the local crystal environment between the two phases[37]. Our calculation shows that brookite-TiO_2 also has a direct band gap of 2.356 eV at G, which is larger than both rutile-TiO_2 and anatase-TiO_2, close to the calculated value of 2.20 eV reported by Mo *et al.*[37].

The general features of density of states for rutile-TiO_2, anatase-TiO_2 and brookite-TiO_2 are quite similar shown in Fig. 3. It is seen that just below the Fermi level the major contributions to the occupied parts come from the O *p* states and the Ti *d* states, with only a small contribution of the Ti *s* and *p* states. Just above the Fermi level the states of O *p* and Ti *d* dominates, while there are few contributions of the O *s* and Ti *s p* states. In other words, both the valence band and conduction band contain contributions from O *p* and Ti *d* predominantly, indicating hybridization between these states, which also means that transitions across the band gap will involve both O *p* and Ti *d* states. Therefore, both of these bands are involved in bonding. The valence band (VB) originates mainly from the bonding between the O *p* and Ti *p* states in the form of *p d* hybridization. The only difference appears to be the four major peaks at -5.24 eV, -4.32 eV, -2.41 eV and -1.26 eV for rutile-TiO_2 and at -4.83 eV, -4.07 eV, -2.36 eV and -1.19 eV for anatase-TiO_2, the triple peaks at -4.29 eV, -2.05 eV and -1.31 eV and the two shoulders located at -4.76 eV, -2.85 eV for brooktie-TiO_2 in the VB, the five major peaks at 3.04 eV, 3.89 eV, 4.92 eV, 5.78 eV, 6.74 eV and a shoulder located at 2.22 eV for rutile-TiO_2, the single-peak at 2.94 eV and a shoulder located at 3.68 eV for anatase-TiO_2 and the single-peak at 2.91 eV for brooktie-TiO_2 in the conduction band.

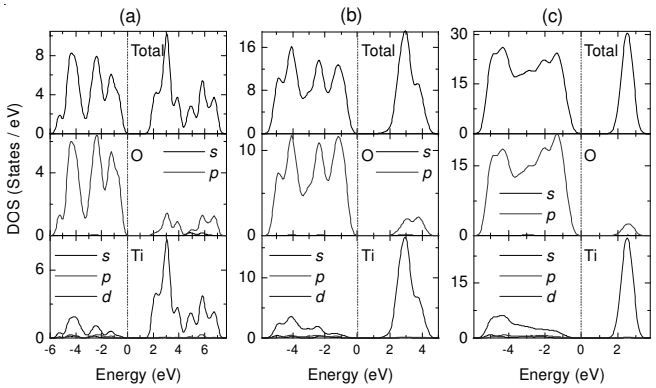

Fig. 3. Total and partial densities of states (PDOS) for (a) rutile-TiO_2, (b) anatase-TiO_2 and (c) brookite-TiO_2. The Fermi level is set to zero

The calculated values of the valence bands width for rutile-TiO_2, anatase-TiO_2 and brookite-TiO_2 are 5.67 eV, 4.64 eV and 4.79 eV respectively, which are in excellent agreement with the experimental value of 5.4 eV[38] and 4.7 eV[39], respectively and the total width of valence band for brookite-TiO_2 is close to that for anatase-TiO_2.

Optical properties: In spite of numerous experimental and theoretical studies of the electronic structure of rutile-TiO_2 and anatase-TiO_2 in recent years, there is only one detailed theoretical investigation of its optical properties[6,11,14,35,40]. For brookite-TiO_2, few limited theoretical works have emerged, but no existing experimental studies can be located. In this section, we will present our results of first principles optical calculations for the three TiO_2 isomers.

The optical properties of TiO_2 isomers are determined by the dielectric function $\varepsilon(\omega) = \varepsilon_1(\omega) + i\varepsilon_2(\omega)$, which is mainly contributed from the electronic structures. The dielectric function is a very important parameter for a material because it is the fundamental feature of the linear response to an electromagnetic wave and determines uniquely the propagation behaviour of the radiation within. The imaginary part $\varepsilon_2(\omega)$ of the dielectric function could be calculated directly from the electronic structure through the joint density of states (DOS) and the momentum matrix elements between the occupied and unoccupied wave functions:

$$\varepsilon_2(\omega) = \frac{ve^2}{2\pi hm^2\omega^2}\int d^3k \sum_{n,n'}\left|\left\langle \vec{k}n\middle|\vec{p}\middle|\vec{k}n'\right\rangle\right|^2 \times f(\vec{k}n)(1-f(\vec{k}n'))\times\delta(E_{\vec{k}n}-E_{\vec{k}n'}-h\omega) \quad (1)$$

where, $h\omega$ is the energy of the incident photon, $\vec{p}$ is the momentum operator $(h/i)(\partial/\partial x)$, $\left|\vec{k}n\right\rangle$ is the eigen function with eigen value $E_{\vec{k}n}$ and $f(\vec{k}n)$ is the Fermi distribution function. The evaluation of the matrix elements of the momentum operator in eqn. (1) is done over the muffin tin and the interstitial regions separately. A full detailed description of the evaluation of these matrix elements is given by Ambrosch-Draxl and Sofo[41].

The real part $\varepsilon_1(\omega)$ of the dielectric function can be evaluated from $\varepsilon_2(\omega)$ using the Kramer-Kronig relations[42]:

$$\varepsilon_1(\omega) = 1 + \frac{2}{\pi}\int_0^\infty \frac{\varepsilon_2(\omega')d\omega'}{\omega'^2-\omega^2}$$

We could also calculate the other optical properties, such as reflectivity $R(\omega)$, absorption coefficient $\alpha(\omega)$, the real part of the refractive index $n(\omega)$, the imaginary part of the refractive index $k(\omega)$ and energy-loss spectrum $L(\omega)$ from $\varepsilon_1(\omega)$ and $\varepsilon_2(\omega)$[19,43]:

$$R(\omega) = \left|\frac{\sqrt{\varepsilon_1(\omega)+j\varepsilon_2(\omega)}-1}{\sqrt{\varepsilon_2(\omega)+j\varepsilon_2(\omega)}+1}\right|^2$$

$$\alpha(\omega) = \sqrt{2}\omega\left[\sqrt{\varepsilon_1^2(\omega)+\varepsilon_2^2(\omega)}-\varepsilon_1(\omega)\right]^{1/2}$$

$$n(\omega) = \left[\sqrt{\varepsilon_1^2(\omega)+\varepsilon_2^2(\omega)}+\varepsilon_1(\omega)\right]^{1/2}/\sqrt{2}$$

$$L(\omega) = \varepsilon_2(\omega)/\left[\varepsilon_1^2(\omega)+\varepsilon_2^2(\omega)\right]$$

The imaginary part of the dielectric function $\varepsilon_2(\omega)$ shown in Fig. 4, directly obtained from the electronic structure calculations, which is the pandect of the optical properties for the three different phases of the TiO_2. For rutile-TiO_2, there are three major peaks located at 3.34, 6.09 and 12.5, which correspond to the three intrinsic plasma frequencies. The peak at 3.34 eV originates from the electronic transition between the O *p* states in the upper valence band and the Ti *s* states in the lowest conduction band, which is close to the calculated band gap (1.85 eV). The peak at 6.09 eV may be due to the transition between Ti *d* and O *p* states in the valence band. The transition between Ti *d* and O *s* states (which are not plotted in the electronic structure) results in the weak peak at 12.5 eV. For anatase-TiO_2, two main peaks exist at 4.23 eV and 7.21eV. For brookite-TiO_2, only one main peak is at 3.93 eV, while a shoulder is at around 7.03 eV. The peak from 7.03 eV to 6.60 eV originates mainly from the transition between Ti *d* and O *p* states. The peak in the low region (from 0.59 eV to 0.76 eV) comes from the electronic transition the O *p* states in the upper valence band and the Ti *s* states in the lowest conduction band.

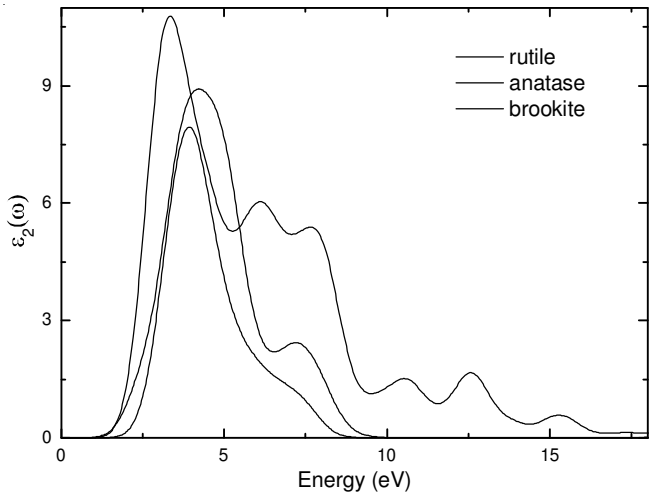

Fig. 4. Imaginary part of dielectric functions ($\varepsilon_2(\omega)$) of TiO_2 polymorphs

The real part of the dielectric function $\varepsilon_1(\omega)$, reflectivity $R(\omega)$ and absorption coefficient $\alpha(\omega)$, the real part of the refractive index $n(\omega)$, the imaginary part of the refractive index $k(\omega)$ and the energy-loss spectrum $L(\omega)$ of TiO_2 are plotted in

Fig. 5. The $\varepsilon_1(\omega)$ of anatase-TiO_2 and brookite-TiO_2 phases are quite similar, having smooth peaks at 2.96 eV, while an obvious peak of them could be found below zero at 5.61 eV and 5.05 eV, where the material behaves like a metallic property. The $\varepsilon_1(\omega)$ of rutile-TiO_2 has two major peaks located at 2.46 eV, 5.54 eV and a shoulder at 6.89 eV, reaching the minimization at 8.55 eV, showing a similar metallic nature. The results for the real part of the dielectric function $\varepsilon_1(0)$, for the three isomers are given in Fig. 5(a). One can see that these curves have a main peak around 2.46 eV for rutile-TiO_2, 2.99 eV for anatase-TiO_2 and 2.98 for brookite-TiO_2 and a minimum between 5.0 eV and 9.0 eV. The static dielectric constant $\varepsilon_1(0)$ has been calculated and the value is 7.65eV for rutile-TiO_2, 5.31 eV for anatase-TiO_2 and 4.01 eV for brookite-TiO_2, respectively. It is noted that a larger energy gap yields a smaller $\varepsilon_1(0)$ value and this could be explained on basis of Penn model[44]. The reflectivity spectrums $R(\omega)$ of the TiO_2 isomers indicate the same reflective ranges from 0 to 25 eV. Moreover, there are two main peaks for the anatase-TiO_2 at 5.06 eV and 9.10 eV, which could be interpreted as the interband transitions and the electron transitions from the valence to conduction bands, respectively. The R (ω) of the rutile-TiO_2 and brookite-TiO_2 have a series of small peaks from 0 eV to 20 eV. The absorption coefficient $\alpha(\omega)$ of the brookite-TiO_2 is narrower than that of the other two polymorphs, ranging from 1.48 to 9.17, from 1.48 to 10.64 and from 1.48 to 22.08 for the three isomers, respectively. In the dispersion curve of the refractive index $n(\omega)$ and $k(\omega)$, all the three polymorphs lie in the regime of normal dispersion in the range from 0 to 10.68 eV and anomalous dispersion from 10.68 eV to 18 eV. The rutile-TiO_2 still exhibits different features from the others in the high-energy region. Besides, we use the electron energy-loss function $L(\omega)$ to describe the energy loss of a fast electron traversing in a certain material and the characteristic associated with the plasma resonance could be represented by the peaks of $L(\omega)$ spectra. The Plasmon peak shows the collective excitation of the loosely bound valence electrons into the unoccupied energy levels in the conduction bands. The positions of peaks in $L(\omega)$ spectra, corresponding to the plasma frequency, indicate the transition from the metallic property $[\varepsilon_1(\omega) < 0]$ to the dielectric property $[\varepsilon_1(\omega) > 0]$ for a material. In addition, the peaks of $L(\omega)$ point out the trailing edges in the reflection spectra, for instance, the peaks of $L(\omega)$ for the rutile-TiO_2, anatase-TiO_2 and brookite-TiO_2 are at 13.38, 10.72 and 9.17 eV, respectively, which correspond to the abrupt reduction in $R(\omega)$.

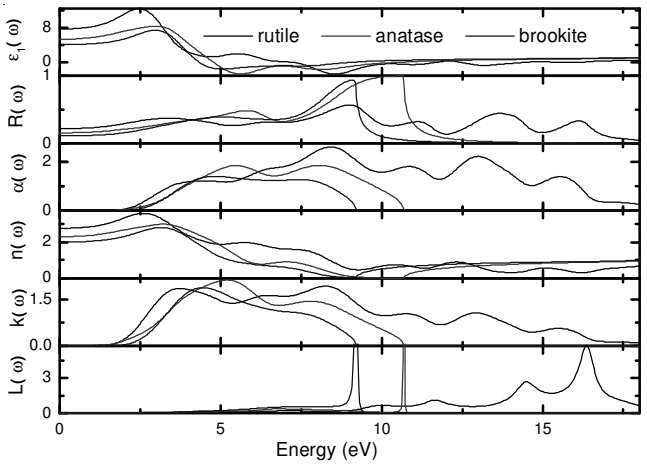

Fig. 5. Real part of the dielectric function $\varepsilon_1(\omega)$, reflectivity $R(\omega)$, absorption coefficient $\alpha(\omega)$, real part of the refractive index $n(\omega)$, imaginary part of the refractive index $k(\omega)$ and electron energy-loss functions $L(\omega)$ for TiO_2

Conclusion

We have presented the results of the first-principles studies of the electronic and optical properties of three isomers of TiO_2. In particular, a basis optimization procedure has been implemented in the present calculation. For ground-state properties, a number of important electronic parameters such as band-widths, band gaps and densities of states have been obtained. Except for the band-gap values, the electronic parameters for the three polymorphs are similar. Our calculated results are consistent with experimental values and a few other previous theoretical calculations.

In summary, both of the valence band and conduction band contain contributions from the states of O *p* and Ti *d*, indicating hybridization between these states. Therefore, both of O *p* and Ti *d* states are involved in bonding. The absorption edges in the calculated spectrum coincide with the band gap energies and the absorption peaks between 2 eV and 9 eV correspond to the band-to-band transitions from O *p* states to Ti *d* states. The states of O *p* and the Ti *d* play major roles in these optical transitions and the values of increase as the band-gap decreases.

ACKNOWLEDGEMENTS

This work was supported in part by the Fundamental Research Funds for the Central Universities (CDJXS10131154) and a Distinguished Ph.D. award from Ministry of Education of China. One of the authors (Wen Zeng) thanks the Chinese Scholarship Council (CSC) project (LJC20093012) for scholarship support.

REFERENCES

1. B.O. Regan and M. Gratzel, *Nature*, **353**, 737 (1991).
2. J.H. Braun, *J. Coat. Technol*., **69**, 59 (1997).
3. M. Subramanian, S. Vijayalakshmi, S. Venkataraj and R. Jayavel, *Thin Solid Films*, **516**, 3776 (2008).
4. M. Lazzeri, A. Vittadini and A. Selloni, *Phys. Rev. B*, **63**, 155409 (2001).
5. K. Tsutsumi, O. Aita and K. Ichikawa, *Phys. Rev. B,* **15**, 4638 (1977).
6. L.A. Grunese, R.D. Leapman, C.N. Wilker, R. Hoffman and A.B. Kunz, *Phys. Rev. B*, **25**, 7157 (1982).
7. K.M. Glassford and J.R. Chelikowsky, *Phys. Rev. B,* **46**, 1284 (1992).
8. D. Vogtenhuber, R. Podloucky, A. Neckel, S.G. Steinemann and A.J. Freeman, *Phys. Rev. B,* **49**, 2099 (1994).
9. J.W. Halley, M.T. Michalewicz and N. Tit, *Phys. Rev. B,* **41**, 1065 (1990).
10. B.W. Veal and A.P. Paulikas, *Phys. Rev. B.* **31**, 5399 (1985).
11. L. Xu, C.Q. Tang, J. Qian and Z.B. Huang, *Appl. Surf. Sci*., **256**, 2668 (2010).
12. H. Weng, X. Yang, J. Dong, H. Mizuseki, M. Kawasaki and Y. Kawazoe, *Phys. Rev. B,* **69**, 125219 (2004).
13. R. Asahi, Y. Taga, W. Mannstadt and A.J. Freeman, *Phys. Rev. B,* **61**, 7459 (2000).
14. S.M. Baizaee and N. Mousavi, *Physica B,* **404**, 2111 (2009).
15. G. Kresse and J. Furthmüller, *Phys. Rev. B,* **54**, 11169 (1996).
16. G. Kresse and J. Hafner, *Phys. Rev. B,* **47**, 558 (1993).
17. P.E. Blöchl, *Phys. Rev. B,* **50**, 17953 (1994).
18. J.P. Perdew, J.A. Chevary, S.H. Vosko, K.A. Jackson, M.R. Pederson, D.J. Singh and C. Fiolhais, *Phys. Rev. B,* **46**, 6671 (1992).

19. H.J. Monkhorst and J.D. Pack, *Phys. Rev. B,* **13**, 5188 (1976).
20. M. Methfessel and A.T. Paxton, *Phys. Rev. B,* **40**, 3616 (1989).
21. O. Jepson and O.K. Andersen, *Solid State Commun*., **9**, 1763 (1971).
22. P.E. Blöchl, O. Jepsen and O.K. Andersen, *Phys. Rev. B,* **49**, 16223 (1994).
23. M.C. Payne, M.P. Teter, D.C. Allan, T.A. Arias and J.D. Joannopoulos, *Rev. Mod. Phys*., **64**, 1045 (1992).
24. R.P. Feynman, *Phys. Rev*., **56**, 340 (1939).
25. A. Fahmi and C. Minot, *Phys. Rev. B,* **47**, 11717 (1993).
26. J. Akimoto, Y. Gotoh, Y. Oosawa, N. Nonose, T. Kumagai, K. Aoki and H. Takei, *J. Solid State Chem*., **113**, 27 (1994).
27. J.K. Burdet, T. Hughbanks, G.J. Mille and J.V. Smith, *J. Am. Chem. Soc*., **109**, 3639 (1987).
28. L. Kavan, M. Gratzel, S.E. Gilbert, C. Klemenz and H.J. Scheel, *J. Am. Chem. Soc*., **118**, 6716 (1996).
29. K.C. Mishra, K.H. Johnson and P.C. Schmidt, *J. Phys. Chem. Solids*, **54**, 237 (1993).
30. G. Shao, *J. Phys. Chem. C,* **112**, 18677 (2008).
31. M.S. Hybertsen and S.G. Louie, *Phys. Rev. B,* **34**, 5390 (1986).
32. F. Bechstedt and R. Del Sole, *Phys. Rev. B,* **38**, 7710 (1988).
33. J.P. Perdew and M. Levy, *Phys. Rev. Lett*., **51**, 1884 (1983).
34. Y. Yin, W. Zhang, S.G. Chen and S.Q. Yu, *Mater. Chem. Phys*., **113**, 982 (2009).
35. M.G. Brik, I. Sildos and V. Kiisk, *Physica B,* **405**, 2450 (2010).
36. H. Chang, K. Kong, Y.S. Choi, E. In, Y. Choi, J.-O. Baeg and S.-J. Moon, *Chem. Phys. Lett*., **398**, 449 (2004).
37. D.M. Shang and W.Y. Ching, *Phys. Rev. B,* **51**, 13026 (1995).
38. S.P. Kowalczyk, F.R. Mefeely, L. Ley, V.T. Gritsyna and A. Schirley, *Solid State Commun*., **23**, 161 (1977).
39. R. Sanjinés, H. Tang, H. Berger, F. Gozzo, G. Margaritondo and F. Lévy, *J. Appl. Phys*., **75**, 2945 (1994).
40. C. Fu, T. Li, J. Qi, J. Pan, S. Chen and C. Cheng *Chem. Phys. Lett*., **494**, 117 (2010).
41. C. Ambrosch-Draxl and J.O. Sofo, *Comput. Phys. Commun*., **175**, 1 (2006).
42. J.P. Perdew, K. Burke and M. Ernzerhof, *Phys. Rev. Lett*., **77**, 3865 (1996).
43. D. Vanderbilt, *Phys. Rev. B,* **41**, 7892 (1990).
44. D.R. Penn, *Phys. Rev*., **128**, 2093 (1962).